NeuroImage 327 (2026) 121722

Contents lists available at ScienceDirect

NeuroImage

journal homepage: www.elsevier.com/locate/ynimg

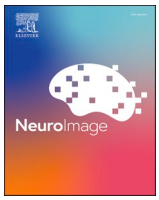

Brain activity inhibition during Short Video Viewing: neurochemical insights

Tiantian Hong [a,1], Conghui Su [a,b,1], Hui Zhou [c], Fengji Geng [d], Yuzheng Hu [a,c,e,*]

[a] Department of Psychology and Behavioral Sciences, Zhejiang University, Hangzhou 310058, China
[b] Faculty of Life and Health Sciences, Shenzhen University of Advanced Technology, Shenzhen 518107, China
[c] The State Key Lab of Brain-Machine Intelligence, Zhejiang University, Hangzhou 310058, China
[d] Department of Curriculum and Learning Sciences, Zhejiang University, Hangzhou 310058, China
[e] MOE Frontiers Science Center for Brain Science & Brain-Machine Integration, Zhejiang University, Hangzhou 310058, China

ARTICLE INFO

Keywords:
Short video viewing
Dorsal anterior cingulate cortex
Dorsolateral prefrontal cortex
Glutamate
Deactivation
Magnetic resonance spectroscopy
Cognitive control
Functional connectivity
Functional magnetic resonance imaging
Social media

ABSTRACT

Cognitive control enables individuals to adapt to the ever-changing environmental demands. The dorsal anterior cingulate cortex (dACC) and the dorsolateral prefrontal cortex (dlPFC) are key regions of the cognitive control network, activated during cognitively demanding tasks. In contrast, the entertaining and habitual nature of short-video consumption for leisure shifts neural processing toward emotional engagement and immediate gratification, contributing to excessive use and diminished self-control in some individuals. This raises a critical question: Does short-video viewing suppress cognitive control regions, and what neurochemical factors may underlie individual differences in this process? To address this question, this preregistered study used proton magnetic resonance spectroscopy (^{1}H-MRS) to measure glutamate and γ-aminobutyric acid (GABA) concentrations in the dACC at rest, and employed functional magnetic resonance imaging (fMRI) to examine dACC and dlPFC activity during free viewing of short videos in 56 young adults. We found that both the dACC and the dlPFC exhibited significant deactivation in response to preferred videos that were watched to completion, compared to less-preferred videos that were terminated early. Moreover, resting-state glutamate levels in the dACC were associated with the magnitude of this deactivation, with higher glutamate concentrations associated with less suppression of both dACC and dlPFC activity. Additionally, functional connectivity between the dACC and dlPFC increased during video viewing, particularly for preferred videos. By integrating fMRI with ^{1}H-MRS, our study provides novel evidence that immersive viewing of preferred short videos deactivates the cognitive control network and that individual differences in this deactivation are linked to glutamate metabolism. These findings enhance our understanding of how digital media consumption interacts with neurochemical processes to influence self-regulation. Our study offers new insights into the neural mechanisms underlying short-video engagement and has implications for understanding excessive digital media use.

1. Introduction

Cognitive control plays a crucial role in balancing immediate gratification with long-term goals, and its impairments are associated with various disorders such as depression (Andrews & Thomson, 2009), anxiety (Maner & Kenrick, 2010), ADHD (Swanson et al., 2002) and addiction (Baler & Volkow, 2006). However, modern digital environments, particularly short-video platforms, provide highly engaging and automated viewing experiences that may shift neural processing away from cognitive control toward gratification-driven mechanisms, reinforcing impulsive consumption and diminishing self-control in some individuals (Cheng et al., 2023; N. Zhang et al., 2023). Consistent with this notion, converging behavioral evidence indicates that both internet addiction and smartphone addiction are reliably associated with diminished self-control capabilities (Ding et al., 2022; Geng et al., 2021). Neuroimaging evidence further demonstrates disruptions in circuits supporting reward processing and cognitive control—including the anterior cingulate cortex, insula, and amygdala—as well as executive regions such as the prefrontal cortex in adolescents and young adults with various behavioral addictions (Áfra et al., 2024; León Méndez et al.,

* Corresponding author.
E-mail address: huyuzheng@zju.edu.cn (Y. Hu).
[1] Tiantian Hong and Conghui Su contributed equally to this work

https://doi.org/10.1016/j.neuroimage.2026.121722
Received 29 May 2025; Received in revised form 6 December 2025; Accepted 13 January 2026
Available online 14 January 2026

2024). Individuals who frequently engage in habitual social media checking behaviors show reduced neural sensitivity in the ventral striatum, amygdala, and dorsolateral prefrontal cortex during anticipation of social rewards (Maza et al., 2023). Concurrently, stronger functional connectivity between the reward system and the prefrontal cortex has been observed in individuals with higher levels of mobile technology engagement, indicating enhanced coupling between reward valuation and cognitive control during habitual media use (Morris et al., 2023). Together, these findings suggest a maladaptive reconfiguration of reward-control interactions, characterized not by heightened reward sensitivity per se, but by weakened top-down regulation alongside increasingly automatized processing.

Immersive and pleasurable media activities, such as playing video games (Michailidis et al., 2018) or watching engaging films (Rigby et al., 2016), can elicit a flow state, marked by intense concentration, altered time perception, and reduced self-consciousness (Michailidis et al., 2018). Faster immersion rates further predict longer viewing times (Lin et al., 2022). A defining feature of the flow state is increased automatization of task performance (Alameda et al., 2022), is neurobiologically accompanied by a U-shaped pattern of medial prefrontal cortex and ventral striatum activity, with pronounced deactivation relative to boredom or overload (Ulrich et al., 2016, 2022). Taken together, these converging lines of evidence indicate that immersive media is associated with reduced prefrontal monitoring. Short-video platforms, characterized by rapid, algorithmically curated, and largely passive content streams, represent an especially potent form of such media and may robustly induce these neurocognitive shifts, potentially suppressing the prefrontal–cingulate cognitive control network.

Given this reduced prefrontal-cingulate engagement during immersive media consumption, it is essential to consider the functional roles of the dorsal anterior cingulate cortex (dACC) and dorsolateral prefrontal cortex (dlPFC) —the core nodes of the cognitive control network. The dACC plays a central role in cognitive control and is involved in reward-based decision-making, conflict monitoring, task difficulty prediction, and signal integration (Babür et al., 2024; Clairis et al., 2024; Clairis & Lopez-Persem, 2023; Ritz & Shenhav, 2024; Sheth et al., 2012; Woo et al., 2022). These functions are typically assessed using tasks such as the Stroop, Go/noGo, and Flanker, which elicit robust dACC activation (Fu et al., 2022; Lesage et al., 2020). Relatedly, reduced dACC activation has been shown to be associated with impairment in cognitive control (Le et al., 2021; Luijten et al., 2014), and cryogenic deactivation of the dACC in macaques results in poorer cognitive control performance (Ma et al., 2019). Given its structural connections with the dACC (Haber et al., 2022; Petrides & Pandya, 1999), the dlPFC regulates cognitive control through its interaction with the dACC (Botvinick & Braver, 2015; Heilbronner & Hayden, 2016). This interaction is mediated by theta-band oscillatory synchrony, facilitating the transmission of feedback-related signals from the dACC to the dlPFC (Helfrich & Knight, 2016; Smith et al., 2015; Voytek et al., 2015; Widge et al., 2019). Together, these two regions play a coordinated role in cognitive control, with the dACC detecting conflicts and evaluating effort allocation, while the dlPFC executes top-down control.

While most research on the role of dACC in cognitive control has focused on its activation, relatively less attention has been given to conditions involving its deactivation or suppression. The dACC typically exhibits increased activation in response to heightened cognitive effort demands compared to baseline (Aben et al., 2020; Shenhav et al., 2016; Silvestrini et al., 2023). However, our previous study (Su et al., 2021) demonstrated that passively viewing personalized short videos suppresses the dACC. Given the dACC's critical role in monitoring, it is plausible that the dACC remains engaged even during rest periods between cognitively demanding tasks. Yet, when individuals engage in low-effort activities, such as watching entertaining short videos, the dACC's monitoring and effort-evaluation functions may be down-regulated compared to rest periods, potentially leading to poor time management and excessive consumption.

Previous research suggests that dACC activation varies across individuals, potentially contributing to differences in cognitive control abilities. Importantly, the dACC activation is influenced not only by task states but also by trait-related factors and regional neurotransmitter concentrations (Yücel et al., 2007). A growing body of multimodal ^{1}H-MRS-fMRI research has demonstrated robust associations between local neurotransmitter levels and task-evoked blood oxygen level-dependent (BOLD) responses (Ip et al., 2017; Kiemes et al., 2021). For example, glutamate concentrations in the anterior cingulate cortex (ACC) have been shown to positively correlate with ACC activation during cognitive control tasks (Cadena et al., 2018), whereas GABA concentrations have been linked to negative BOLD responses in the ACC (Northoff et al., 2007). Notably, however, these metabolite–BOLD relationships appear to be context dependent: they are relatively consistent in emotion-related paradigms but show greater variability in cognitive control and working memory tasks (Overbeek et al., 2019; Yücel et al., 2007).

Beyond regional activation, neurotransmitter concentrations also contribute to large-scale network coupling (Finkelman et al., 2025; Mohammadi et al., 2025; Mouchlianitis et al., 2023). Higher ACC glutamate levels have been associated with greater task-induced deactivation of the default mode network (De Joode et al., 2023; Falkenberg et al., 2012; Hu et al., 2013; Overbeek et al., 2019). Similarly, GABA levels in the dACC and prefrontal cortex have been linked to BOLD responses in distal regions such as the putamen and cerebellum during reward learning and emotion processing (Finkelman et al., 2025; Oboshi et al., 2025). More broadly, the local excitation–inhibition (E/I) balance—regulated primarily by glutamate and GABA—is thought to shape both regional activation patterns and distributed network dynamics (Hegarty et al., 2018). Building on this body of work, the present study investigates how resting-state glutamate and GABA concentrations in the dACC modulate its activity and functional connectivity during naturalistic short-video viewing—a common yet underexplored context in neurochemical research. This approach advances mechanistic understanding of how regional neurochemistry influences cognitive-control network dynamics under real-world conditions.

While previous studies have explored the neural mechanisms of self-regulation through cognitive tasks that activate the dACC and dlPFC, few have directly examined how the cognitive control network responds to engaging, entertainment-based activities that often lead to self-regulation failure in some individuals. This gap raises a critical question: Does short-video viewing suppress cognitive control regions, and what neurochemical mechanisms underlie individual differences in this process? To address these critical issues, we employed ^{1}H-MRS in conjunction with fMRI. This dual-modality approach enables a comprehensive investigation of the relationship between resting-state neurochemical concentrations and task-induced activity in key cognitive control regions, offering deeper insights into the neural basis of short-video consumption and its implications for self-regulation. This study was preregistered on September 20th 2024 (https://aspredicted.org/h4pm2.pdf).

2. Methods

2.1. Participants

In this study, 66 participants with normal or corrected-to-normal vision were recruited through online advertisements. The experimental procedures were approved by the Ethics Committee of Zhejiang University. All participants provided written informed consent before participation and received financial compensation. After applying exclusion criteria, 10 participants were removed from analysis: six due to excessive head motion (maximum displacement $>$ 3 mm) and four due to low-quality MRS spectra (specific exclusion criteria for MRS are detailed in *Section 2.3.3 ^{1}H-MRS data preprocessing*). No participants were excluded for psychiatric disorders, such as depression, anxiety,

schizophrenia, or substance use disorders. The final sample for statistical analyses consisted of 56 participants (mean age = 23.30 ± 2.45 years; 37 males and 19 females). Before fMRI scanning, all participants self-reported their estimated daily short-video viewing time using four categorical levels: less than 30 minutes, 30 minutes to 1 hour, 1 to 2 hours, and more than 2 hours. All participants reported having some degree of short-video use experience (less than 30 min: n = 6; 30 min–1 h: $n = 29$; 1–2 h: $n = 10$; more than 2 h: $n = 11$).

2.2. Short-video viewing task

This study employed a natural video viewing task adapted from our previous study (Su et al., 2023). Participants viewed two 6-minute video blocks separated by 30-second rest intervals (total duration: 815 seconds). The videos were pre-recorded by the experimenter on a smartphone (Xiaomi 9 model) with no prior history of short-video app usage history. The video library consisted of 160 clips spanning five categories: single-person actions, multi-person interactions, pets, game scenes, and natural scenery. The video duration ranged from 7 to 104 seconds (Mean = 23.7 seconds), with 130 clips (81.3 %) under 30 seconds.

Participants were instructed to watch the videos naturally while minimizing head movement. To proceed to the next video, participants could press a button placed in their right hand at any time. Based on their viewing completion, videos were classified as: "Liked" (watched to end), "Disliked" (skipped before 50 % progress), and “Type 3” (skipped after 50 % progress).

Analysis focused on brain activation and connectivity during the "Liked" and "Disliked" conditions. Although the video playback order was fixed, the total number of videos watched varied across participants (Mean = 70.88 ± 28.46, ranging from 42 to 138). On average, participant watched 19.09 ± 8.66 “Liked” videos and 35.77 ± 30.73 “Disliked” videos. A significant difference was observed between the two types of videos ($t(55) = -3.44$, $p = .001$). Video stimuli were delivered via E-Prime 3.0 (psychology software tools, Pittsburgh, PA; https://www.pstnet.com), and displayed on an MRI-compatible screen with a resolution of 720 × 1280 pixels.

2.3. Brain image and ^{1}H-MRS data

2.3.1. Data acquisition

Neuroimaging and ^{1}H-MRS data were acquired using a 3T Siemens Prisma scanner (MAGNETOM Prisma, Siemens Healthcare Erlangen, Germany) equipped with a 20-channel coil at the Center for Brain Imaging Science and Technology (CBIST), Zhejiang University.

High-resolution anatomical images were obtained using a T1-weighted 3D magnetization-prepared rapid gradient echo sequence with the following parameters: TR/TE = 2300/2.32 ms, flip angle = 8°, FOV = 240 × 240 mm^2, matrix = 256 × 256, voxel size = 0.94 × 0.94 × 0.9 mm^3, and 208 sagittal slices. Functional images were collected using a T2*-weighted single-shot echo-planner imaging sequence with multiband acceleration (multiband factor = 4). The acquisition parameters were: TR/TE = 1000/34 ms, flip angle = 50°, FOV = 230 × 230 mm^2, matrix = 92 × 92, voxel size = 2.5 × 2.5 × 2.5 mm^3, and slice number = 52.

Prior to MRS scans, automated shimming was performed to optimize static magnetic field homogeneity. Glutamate and GABA concentrations were quantified using a water-suppressed MEGA-PRESS sequence (TE/TR = 68/2000 ms, editing pulses at 1.9 ppm (ON) and 7.5 ppm (OFF), bandwidth = 2000 Hz, acquisition duration = 1024 ms, vector size = 2048, editing pulse bandwidth = 53 Hz) with 72 averages for Cohort 1 (n = 25) and 120 averages for Cohort 2 (n = 31). An MRSinMRS checklist for this study is provided in Table S1 (A. Lin et al., 2021). Data were acquired with identical structural/fMRI parameters and video task protocols across cohorts, except the MRS average number being increased from 72 to 120 to increase signal to noise ratio (SNR). To account for potential systematic SNR variation between the two cohorts, the number of averages was included as a covariate at group-level analyses. Water spectra were also acquired from the same voxel of interest (VOI) using the MEGA-PRESS sequence with five averages for all participants.

For MRS anatomic positioning, a 26 × 21 × 15 mm^3 VOI was manually placed in the bilateral dACC (*Fig. 1A, left*), angled tangentially to the corpus callosum and crossed two hemispheres. A control VOI was placed in the Visual cortex (26 × 21 × 15 mm^3; *Fig. 1A, right*) to isolate cognitive-emotional effects in dACC from stimulus-driven confounds. The visual VOI was placed in the center of the occipital lobe, ensuring that the entire voxel remains within the occipital lobe region to minimize partial volume effect. The center of mass coordinates in standard MNI space ([right, anterior, superior]) were [.74 ± 1.14, 25.40 ± 8.32, 26.69 ± 6.10] and [1.14 ± 1.51, -84.26 ± 2.35, 6.93 ± 2.87] for the dACC and visual VOI, respectively.

2.3.2. fMRI data preprocessing

The fMRI data preprocessing was conducted using AFNI (Cox, 1996), ANTs (http://stnava.github.io/ANTs/), and SPM12 (https://www.fil.ion.ucl.ac.uk/spm/). The pipeline included four primary steps: slice timing correction, motion correction, spatial normalization, and smoothing using a Gaussian kernel with a full-width at half-maximum (FWHM) of 5 mm. Framewise displacement (FD) was calculated for each volume to quantify head motion, following the method described by Power et al. (2012). Rotational displacements were converted from radians by assuming a spherical head model of 50-mm radius. Mean FD was included as a covariate in statistical analyses to control for the potential effects of individual differences in motion-related variance.

The FD for each volume (FD_i) was calculated as:

$$FD_i = \sum_j \left| d_{(i-1)j} - d_{ij} \right|$$

Where j represents the six motion parameters (*x, y, z, pitch, roll, yaw*), and $i = 2, 3, \ldots$

2.3.3. ^{1}H-MRS data preprocessing

MRS data preprocessing was performed using the FID-A toolkit (Simpson et al., 2017). Glutamate concentrations were quantified using LCModel (Provencher, 1993; version 3.6-1H; *Fig. 1B, left*), while GABA concentrations were quantified using Gannet (Edden et al., 2014; *Fig. 1B, right*). LCModel fits experimental spectra in the frequency domain with a combination of basis sets, each representing the frequency spectrum of a specific metabolite, alongside a baseline to account for unmodeled signals. Gannet, a MATLAB-based open-source software, specializes in quantitative GABA analysis using a simple Gaussian model. While LCModel can estimate GABA concentrations, Gannet was selected due to its superior interclass correlation coefficient in prior methodological comparisons (Saleh et al., 2016), ensuring enhanced reliability for GABA analysis.

According to the LCModel Manual, the full width at half-maximum (FWHM) provides a rough estimate of the linewidth in the in vivo spectrum while the signal-to-noise (S/N) is defined as the ratio of the maximum amplitude in the spectrum-minus-baseline within the Analysis Window to twice the root-mean-square of the residuals (S. Provencher, 2021). In GABA fitting, FWHM is calculated as the width of the fitted GABA peak in Hz (Edden et al., 2014). However, these two parameters can only serve as general references for data quality and do not precisely characterize it (S. Provencher, 2021).

In contrast, the Cramer-Rao lower bound (CRLB)—reported as %SD values in LCModel concentration tables and as GABAFitError in Gannet, which represents the standard deviation of the residual of the GABA peak fit expressed as a percentage of the GABA peak amplitude—simultaneously accounts for both spectral resolution and noise level (Kreis, 2004). Therefore, it offers the most useful guidance regarding the reliability of the metabolite concentration estimates. We have provided detailed data quality parameters for both glutamate and GABA in the

two regions of interest in *Table S2*. Consistent with previous studies (Coum et al., 2016; Kanagasabai et al., 2024), glutamate data with CRLB values exceeding 10 % were excluded from subsequent analyses. For GABA, data points with CRLB exceeded 20 % were excluded in accordance with standard practices (Long et al., 2013; Wijtenburg et al., 2013).

2.3.4. ^{1}H-MRS data partial volume correction

Differences in proton densities, T1 and T2 relaxation times across gray matter (GM), white matter (WM), and cerebrospinal fluid (CSF) influence MRS signals. Consequently, the volume fractions of different tissue types were calculated by segmenting T1 images using Gannet (Edden et al., 2014). The water signal was then corrected by the tissue fractions with varying proton density according to a previous study (Geramita et al., 2011). T1 and T2 values of glutamate in WM (T1 = 1170 ms, T2 = 124 ms) and GM (T1 = 1270 ms, T2 = 135 ms) (Ganji et al., 2012; Mlynárik et al., 2001) were used for a global relaxation correction to obtain absolute quantification in millimolar (mM), assuming no contribution to glutamate MR signal from CSF. The proton density ratio of WM to GM of glutamate (0.5) (Choi et al., 2006; Srinivasan et al., 2006) was used to calculate the glutamate concentrations in GM. The correction calculations are outlined in the equation provide by Chen et al. (2019) as below:

$$(S_{met}/S_{wat})_{corr} = (S_{met}/S_{wat})_{uncorr} \cdot \frac{\left(WM\ \%\cdot f_{wat\_WM} + GM\ \%\cdot f_{wat\_GM} + CSF\ \%\cdot f_{wat\_csf}\right)}{\left(WM\ \%\cdot f_{met\_WM} + GM\ \%\cdot f_{met\_GM}\right)}$$

Where S is the metabolite/water signal; WM %, GM % and CSF % are the tissue percentages; f is the sensitivity factor of metabolite/water in a certain tissue type.

2.4. Region of interest (ROI) definition for fMRI analysis

To investigate the neural mechanisms underlying short-video viewing, we focused on two key ROIs: the dACC and the left dlPFC. These regions are widely implicated emotion regulation, attention, and decision-making (Piretti et al., 2022; Silton et al., 2010; Smith et al., 2019).

The dACC mask (Fig.2, *left*) was created using the CoRegister module of Gannet (Edden et al., 2014). Participant-specific masks were then normalized to standard space, and an overlapping mask with at least 90 % coverage across participants was created using 3dMean and 3dcalc. This overlapping mask served as the basis for all subsequent analyses of dACC brain activation and functional connectivity.

For the left dlPFC, we focused on the left portion of Brodmann area 46 (*Fig. 2, middle*), a region wisely recognized for its central role in implementing cognitive control functions (Breukelaar et al., 2017). The primary visual cortex (V1) was designated as the control region. While the MRS visual cortex voxel spanned broader occipital regions, we refined our analyses to Brodmann area 17 to isolate V1-specific activity, ensuring better control over low level visual stimulus confounds (*Fig. 2, right*).

2.5. Statistical analyses

2.5.1. ROIs activation during video-watching task

To examine potential differences in ROI activation between the "liked" and "disliked" conditions during short-video watching, we first performed first-level general linear modeling (GLM) using 3dDeconvolve in AFNI. Three block regressors were constructed to represent the brain's response to different video classifications: "liked," "disliked," and "Type 3". The onset times were defined as the moments when the video appeared on the screen, and the durations corresponded to the lengths of the video being viewed. For the "disliked" and "Type 3" conditions (where participants pressed the button), two additional event-related regressors were included to model the changes in fMRI signals associated with motor responses in these conditions. In addition to the task-related regressors, nuisance regressors included the six head motion parameters, the first five components of CSF and WM (which have been shown to contain physiological noise) (Windischberger et al., 2002), and signal drifts (automatically determined with the -polort A option in the 3dDeconvolve command).

After performing the GLM, brain activation levels (β values) for the dACC, dlPFC, and V1 regions under both the "disliked" and "liked" conditions were extracted. Six separate one-sample t-tests (one for each ROI-condition combination: 3 ROIs x 2 conditions) were conducted to determine whether activations in these models significantly different from baseline. Three paired-sample t-tests (one per ROI) were then performed to compare activation differences between the "disliked" and "liked" conditions within each ROI. To control for multiple comparisons across all nine tests (6 one-sample + 3 paired tests), a Bonferroni correction was applied, resulting in a significance threshold of p = .00555 (.05/9).

We hypothesized that cognitive control-related regions (dACC and dlPFC) would be suppressed during the "liked" condition and undergo disinhibition during the "disliked" condition. In contrast, the V1 region was expected to show significant activation in both conditions, with no significant difference between them.

2.5.2. Task-dependent connectivity between ROIs

To explore how brain connectivity between the dACC and the dlPFC/V1 varies across task conditions, we conducted psychophysiological interaction (PPI) analysis. PPI, as proposed by Friston et al. (1997), examines the interaction between a physiological variable (the time series of a specific brain region) and a psychological variable (task conditions) within a regression model. This method allows the investigation of how connectivity between brain regions differs between specific task conditions.

For each participant, a GLM analysis was performed in AFNI, incorporating the following regressors: five task regressors (three block regressors and two event-related regressors, see *Section 2.5.1 ROIs activation during video-watching task* for details), one regressor representing the time series of the seed region (dACC 90 % overlap mask), three interaction regressors capturing the product of the seed region time series and the task conditions (dACC * disliked, dACC * liked, and dACC * type3), two nuisance regressors for WM and CSF corrections (the first five components of CSF and WM), and six motion regressors to account for head movement.

Using 3dROIstats, we extracted dACC connectivity with the dlPFC and V1 under the "disliked" and "liked" conditions. One-sample t-tests were conducted to evaluate whether connectivity differed significantly from baseline, while paired-sample t-tests were performed to compare connectivity between the two conditions. To account for multiple comparisons, a Bonferroni correction was applied, with the significance threshold set at p = .00833 (.05/6).

We hypothesized that the dACC would exhibit significant positive

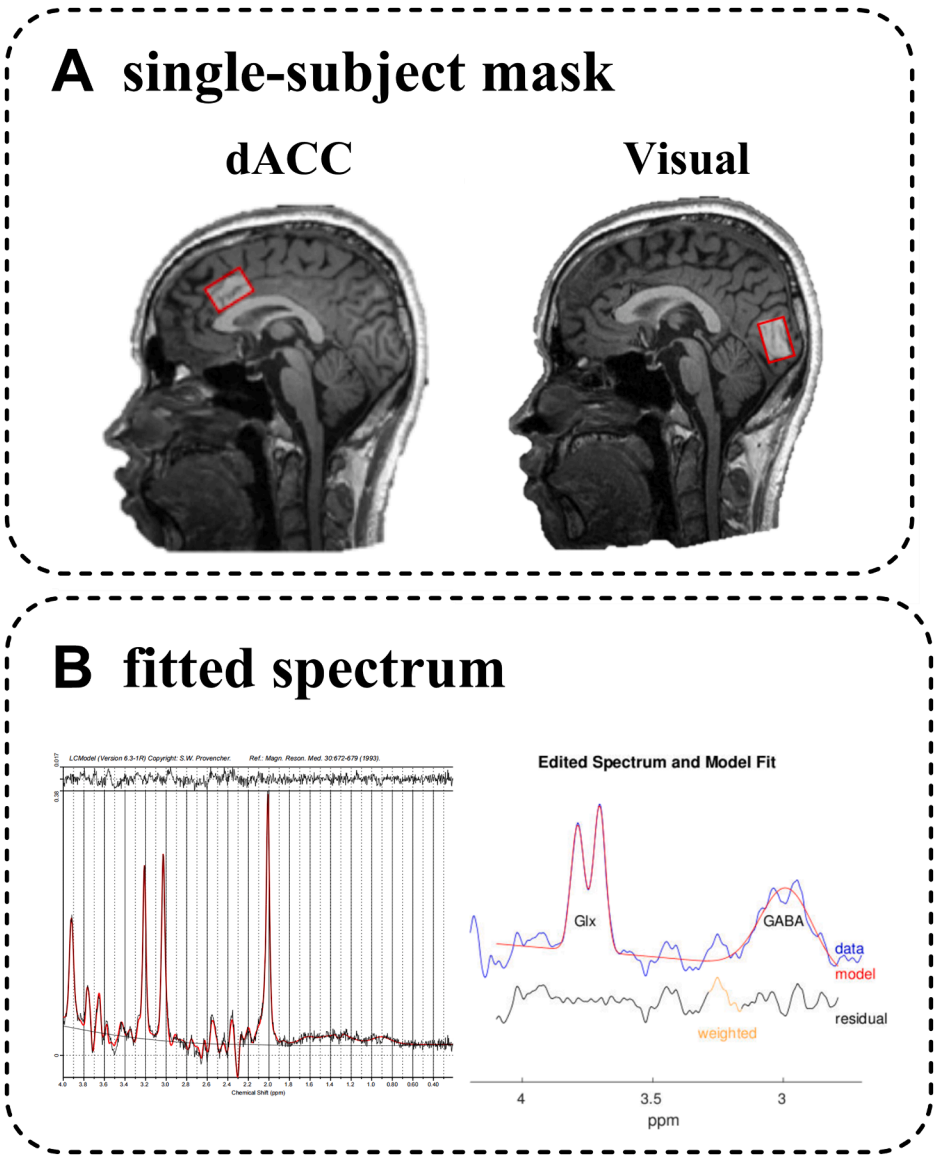

Fig. 1. Placement of MRS Regions of Interest and Spectrum Fitting. Panel (A, left) depicts the placement of a 26 × 21 × 15 mm^3 voxel in the dACC for MRS data collection. The right side of Panel (A) shows the placement of the control region in the visual cortex, which allows for the isolation of cognitive and emotional influences on dACC activity. Glutamate concentrations were quantified using LCModel, with a representative fitted spectrum presented in Panel (B, left). GABA concentrations were quantified using Gannet, and the corresponding fitted spectrum is illustrated in Panel (B, right).

connectivity with the dlPFC under both conditions, with stronger connectivity observed in the "disliked" condition compared to the "liked" condition. In contrast, we anticipated that the dACC would show no significant connectivity with the V1 in either condition, nor significant differences in dACC-V1 connectivity between conditions.

2.5.3. Correlations between glutamate/GABA concentration and ROI activation/connectivity

To investigate the relationship between neurotransmitter concentrations and ROIs activation as well as task-dependent connectivity, we employed hierarchical regression models. These models evaluated the unique contribution of dACC glutamate and GABA concentrations while controlling for relevant covariates. The change in R^2 (ΔR^2) was used as an indicator of the metabolites' contribution to the model.

In Step1, a set of covariates was included: age, gender, number of MRS averages, dACC glutamate CRLB, dACC CSF content, and mean head motion during the short-video watching task. In Step2, dACC glutamate and GABA concentrations were added to the model. The dependent variables were the activations of the dACC, dlPFC, and V1 under "liked" and "disliked" conditions, as well as the connectivity measures between dACC-dlPFC and dACC-V1 under both conditions.

We hypothesized that higher dACC glutamate would be associated with reduced deactivation in the dACC and dlPFC, whereas higher dACC GABA would show the opposite pattern. Furthermore, we hypothesized that both metabolites would be associated with dACC-dlPFC functional connectivity, but would not show significant correlations with V1 activation or dACC-V1 connectivity.

To explore the relationship between metabolites in the visual cortex (control region) and regional activation, we repeated the analysis using the visual cortex metabolites in place of dACC metabolites. Activation values derived from the visual cortex mask (90 % overlap mask) under "liked" and "disliked" conditions served as the dependent variables. We hypothesized that visual cortex glutamate and GABA concentrations would not exhibit significant correlations with visual activation in either condition.

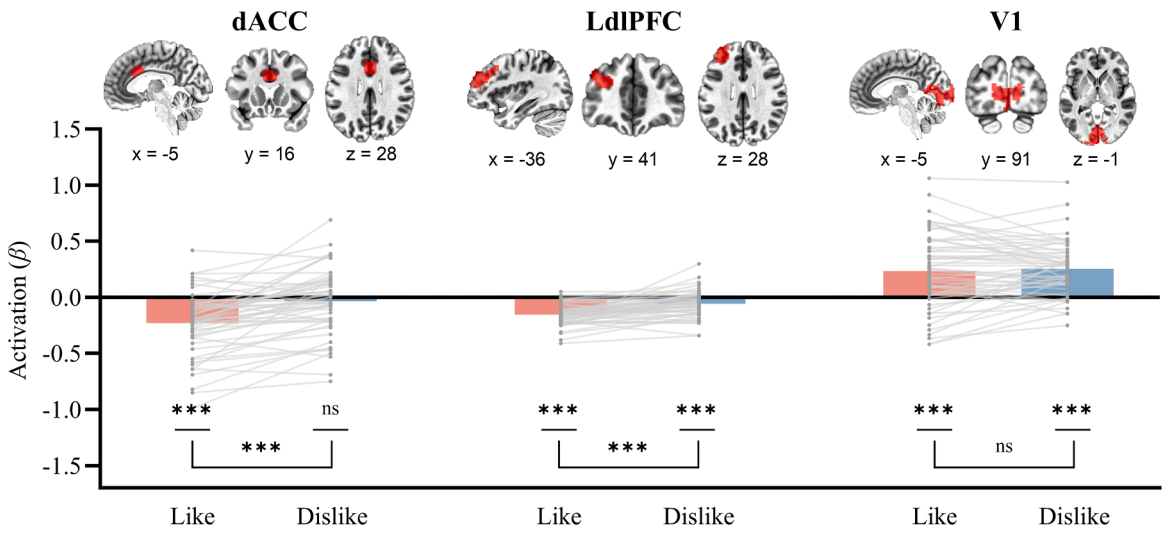

Fig. 2. The dACC and dlPFC showed reduced activation during short-video viewing, whereas the visual cortex exhibited increased activation relative to baseline. The upper portion of the Fig. illustrates the ROIs analyzed in this study: the overlapping dACC region with 90 % participant coverage following alignment (left), the dlPFC extracted from the left portion of Brodmann area 46 (middle), and V1, designated as the control region, extracted from Brodmann area 17 (right).
* $p < .05$, ** $p < .01$, *** $p < .001$

3. Results

3.1. Demographic statistics

The mean corrected dACC glutamate concentration was 10.34 ± 1.00 μM, while the mean corrected dACC GABA concentration was 2.20 ± 1.59 μM. For the visual cortex, after applying a CRLB threshold of 10 % for glutamate and 20 % for GABA, 50 participants remained in the visual-MRS related analysis. The mean corrected visual glutamate concentration was 9.39 ± .90 μM, and the mean corrected GABA concentration was 1.98 ± .41 μM.

3.2. Distinct activation patterns in cognitive control regions during liked and disliked video

As shown in Fig. 2, both the dACC and the left dlPFC demonstrated significant suppression during the viewing of liked videos (dACC: $t(55) = -6.30$, $p < .001$; dlPFC: $t(55) = -12.20$, $p < .001$). In contrast, during the viewing of disliked videos, dACC activation did not differ significantly from baseline ($t(55) = -.90$, $p = .373$), whereas dlPFC activation was significantly lower than baseline ($t(55) = -3.731$, $p < .001$). A direct comparison between conditions indicated that, relative to the disliked condition, both dACC and dlPFC exhibited significantly greater suppression during the viewing of liked videos (liked vs disliked, dACC: $t(55) = -6.52$, $p < .001$; dlPFC: $t(55) = -6.21$, $p < .001$).

In the V1 control region, significant activation was consistently observed across video types (liked: $t(55) = 5.21$, $p < .001$; disliked: $t(55) = 7.76$, $p < .001$), with no significant differences identified between conditions (liked vs disliked, $t(55) = -.65$, $p = .519$). It is important to note that the significance threshold was set at $p = .00555$ (.05/9), following Bonferroni correction.

3.3. dACC glutamate concentration positively correlates with dACC and dlPFC activations

After controlling for age, gender, number of averages, dACC CRLB, dACC CSF content, and mean head motion during video watching, we found that dACC glutamate concentration made a significant contribution, independent of GABA concentration, to dACC activation under both conditions (liked: $\beta = 2.51$, $p = .016$; disliked: $\beta = 2.88$, $p = .006$) and to dlPFC activation in the disliked condition ($\beta = 3.95$, $p < .001$) (Fig. 3). However, no significant relationship was observed between dACC glutamate concentration and dlPFC activation in the liked condition ($\beta = 1.93$, $p = .060$) or V1 activation under either condition (liked: $\beta = 1.52$, $p = .134$; disliked: $\beta = 1.12$, $p = .267$).

In contrast, dACC GABA concentration showed a significant contribution to V1 activation in both conditions (liked: $\beta = 2.50$, $p = .016$; disliked: $\beta = 3.16$, $p = .003$) but was not significantly associated with dACC (liked: $\beta = 2.01$, $p = .050$; disliked: $\beta = 1.54$, $p = .129$) or dlPFC activation (liked: $\beta = .09$, $p = .931$; disliked: $\beta = .15$, $p = .881$). Contributions of other parameters to the models are detailed in Table 1,2 and *Table S3*.

In addition to acquiring MRS data from the dACC region, we also placed a region of interest in the occipital lobe to estimate glutamate and GABA concentrations in the visual cortex, which served as a control region (Fig. 1*A, right, N* = 50). Analysis of the relationship between visual metabolite concentrations and regional activation revealed no significant correlations between visual glutamate and GABA concentrations and visual activation in either the "liked" or "disliked" conditions (*Table S6*).

3.4. Increased connectivity between dACC and dlPFC during viewing: more pronounced increase during "liked" videos

We analyzed the connectivity between the dACC and dlPFC/V1 and further assessed its relationship with dACC metabolites, specifically glutamate and GABA concentrations. As depicted in Fig. 4*A*, connectivity between the dACC and left dlPFC was significantly greater than baseline in both conditions (liked: $t(55) = 5.75$, $p < .001$; disliked: $t(55) = 4.65$, $p < .001$), with a significant difference between conditions (liked vs disliked, $t(55) = 2.72$, $p = .009$). Conversely, the connectivity between dACC and V1 control region did not significantly differ from baseline under either condition (*Fig. 4B*; liked: $t(55) = -1.02$, $p = .313$; disliked: $t(55) = -1.85$, $p = .070$), nor was there a significant difference between conditions (liked vs disliked, $t(55) = 1.12$, $p = .267$). The significance threshold was set at $p = .00833$ (.05/6) dACC glutamate and GABA concentrations did not exhibit significant contributions to dACC-dlPFC or dACC-V1 connectivity under either condition, as detailed in *Table S4,5*.

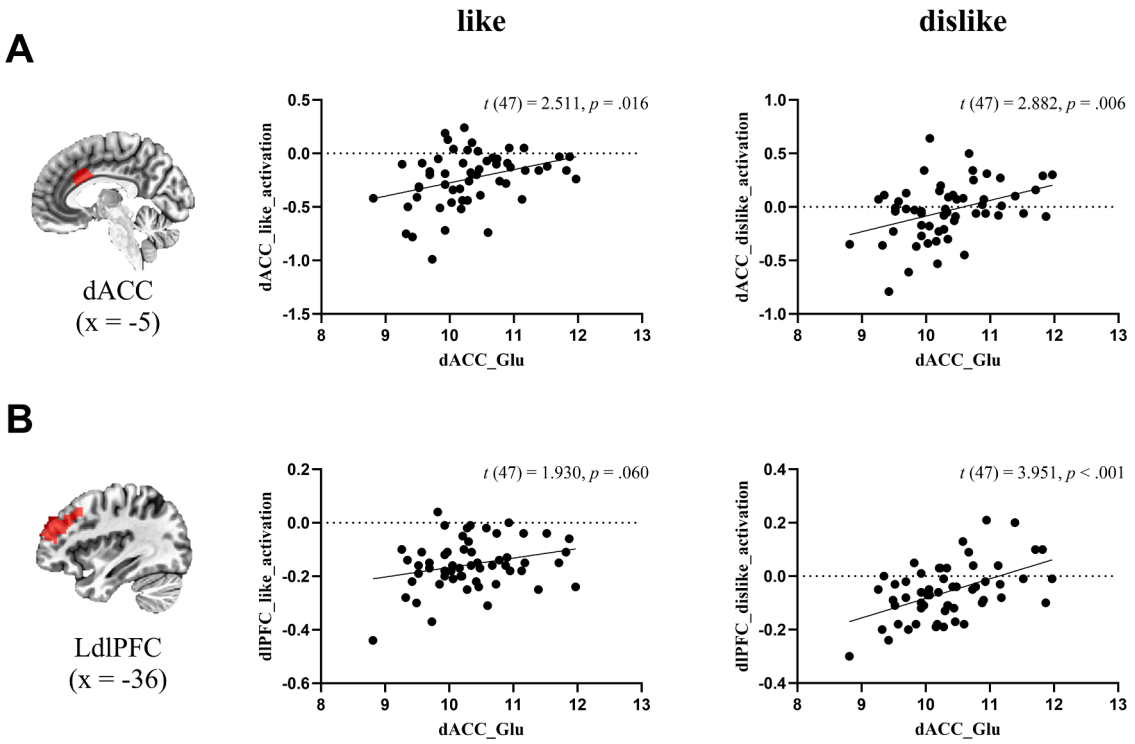

Fig. 3. The dACC glutamate concentration positively correlated with activation levels in both the dACC and dlPFC across the two conditions. Specifically, individuals with higher glutamate concentrations in the "liked" condition exhibited reduced inhibition (less negative activation) in the dACC and dlPFC, while showing greater disinhibition in the "disliked" condition.
To visualize the results of the hierarchical regression analysis, linear regressions were performed with covariates as independent variables. Dependent variables alternated between dACC glutamate concentrations and activations extracted from the ROIs under both "liked" and "disliked" conditions. Residuals from these models were calculated and added to the respective group means of dACC glutamate and ROI activations. Scatter plots were generated to depict the relationship between adjusted dACC glutamate concentrations and ROI activations, with significance levels denoted as * $p < .05$, ** $p < .01$, *** $p < .001$.

Table 1
Summary of hierarchical regression analyses based on dACC metabolites for dACC activation.

	dACC "like" activation								dACC "dislike" activation							
	step1				step2				step1				step2			
Variables	R^2	*B*	*SE*	*β*	△R^2	*B*	*SE*	*β*	R^2	*B*	*SE*	*β*	△R^2	*B*	*SE*	*β*
Covariates	.13								.13							
Age		-.02	.02	1.23						-.00	.02	-.26				
Gender		.06	.09	.67						.13	.09	1.46				
Averages		.05	.09	.61						-.04	.09	-.44				
dACC_crlb		9.81	4.91	2.00						.19	5.10	.04				
dACC_c3		-.09	1.37	-.06						1.14	1.42	.80				
FD_video		.80	.98	.81						1.19	1.02	1.17				
Metabolites					.13*								.14*			
dACC_Glu						.12	.05	2.51*						.15	.05	2.88**
dACC_GABA						.05	.03	2.01						.04	.03	1.54

dACC_crlb, Cramer-Rao lower bound of dACC glutamate data fitting; dACC_c3, dACC cerebrospinal fluid content; FD_video, mean head motion during the short-video watching task; dACC_Glu, dACC glutamate concentration; dACC_GABA, dACC GABA concentration
Gender (male = 1), Averages (Cohort1[120] = 1)
* $p < .05$,
** $p < .01$,
*** $p < .001$

4. Discussion

This study investigated dynamic changes in cognitive control network activity during short video viewing and examined the influence of resting-state metabolite concentrations on task-evoked neural responses. Key findings revealed preference-dependent patterns: when participants viewed "liked" videos, two core regions of the cognitive control network—the dACC and the dlPFC—exhibited significant deactivation. In contrast, during "disliked" video viewing, dACC activity remained comparable to baseline levels, while dlPFC activity remained suppressed. Task-related activity in these regions was correlated with resting-state glutamate (an excitatory neurotransmitter) in the dACC, with no significant association observed for GABA (the primary inhibitory neurotransmitter). Notably, individuals with higher resting-state dACC glutamate concentrations displayed reduced suppression of both dACC and dlPFC activity during video viewing. Additionally, we observed increased dACC-dlPFC functional connectivity during video viewing, particularly for "liked" videos. However, no significant

Table 2
Summary of hierarchical regression analyses based on dACC metabolites for dlPFC activation.

	dlPFC "like" activation								dlPFC "dislike" activation							
	step1				step2				step1				step2			
Variables	R^2	*B*	*SE*	β	$\triangle R^2$	*B*	*SE*	β	R^2	*B*	*SE*	β	$\triangle R^2$	*B*	*SE*	β
Covariates	.04								.18							
Age		-.00	.01	-.71						-.00	.01	-.29				
Gender		-.01	.03	-.41						.05	.04	1.26				
Averages		.01	.03	.16						.04	.04	1.02				
dACC_crlb		-1.83	1.77	-1.03						.14	2.00	.07				
dACC_c3		-.00	.49	-0.00						1.19	.56	2.14*				
FD_video		.06	.36	0.17						.07	.40	.18				
Metabolites					.08								.22***			
dACC_Glu						.04	.02	1.93						.07	.02	3.95***
dACC_GABA						.00	.01	0.09						.00	.01	.15

dACC_crlb, Cramer-Rao lower bound of dACC glutamate data fitting; dACC_c3, dACC cerebrospinal fluid content; FD_video, mean head motion during the short-video watching task; dACC_Glu, dACC glutamate concentration; dACC_GABA, dACC GABA concentration
Gender (male = 1), Averages (Cohort1[120] = 1)
* $p < .05$,
** $p < .01$,
*** $p < .001$

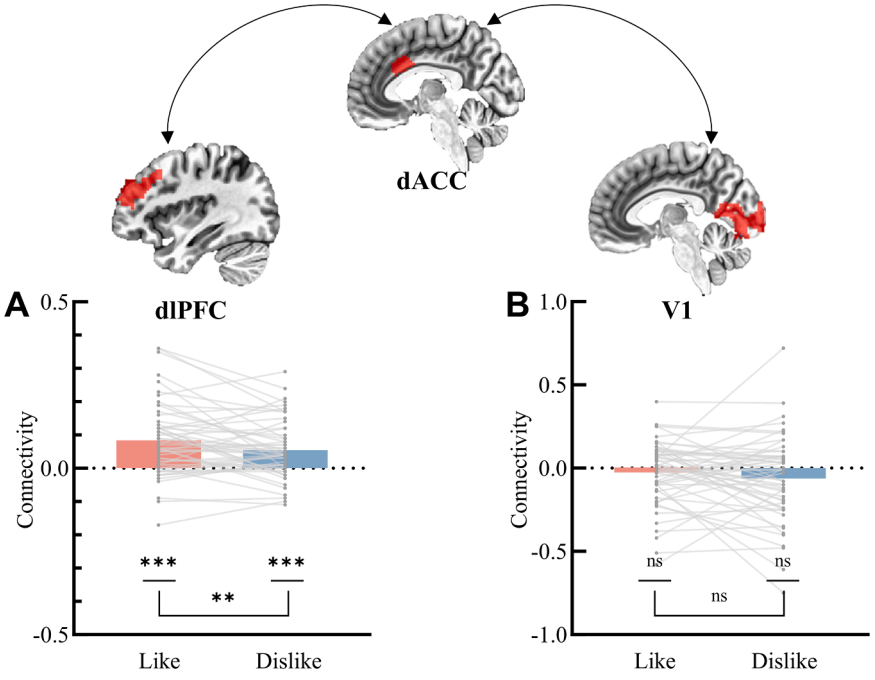

Fig. 4. The connectivity between the dACC and left dlPFC (A) was significantly greater than baseline in both conditions, with a notable difference between the two conditions. In contrast, the connectivity between dACC and V1 control region (B) did not show a significantly deviation from baseline in either condition, and no significant difference was observed between the conditions.
* $p < .05$, ** $p < .01$, *** $p < .001$

relationship was identified between metabolite concentrations and functional connectivity. Together, these results advance our understanding of the interplay between regional neurochemistry and large-scale network dynamics, revealing novel evidence that excitatory neurotransmission is closely linked to the modulation of cognitive control during emotionally salient experiences.

4.1. Adaptive cognitive control during short video viewing: the role of dACC and dlPFC in deactivation

The dACC and dlPFC—structurally interconnected regions critical for behavioral adaptation (Haber et al., 2022; Petrides & Pandya, 1999)—collaboratively regulate cognitive control (Botvinick & Braver, 2015; Heilbronner & Hayden, 2016). The conflict monitoring hypothesis posits that the dACC detects conflicts and recruits the dlPFC to resolve them (Carter et al., 1998; Kerns et al., 2004). In tasks requiring active conflict resolution (e.g., Stroop tasks), both regions typically activate robustly (Mohanty et al., 2007; Song et al., 2017). However, during "liked" short video viewing, we observed significant deactivation in both regions. Importantly, this deactivation should not be interpreted as a failure of cognitive control capacity. Rather, it likely reflects the low conflict inherent to passive viewing, reducing demands on top-down cognitive control mechanisms.

Two considerations help clarify the nature of the observed deactivation. First, reduced task engagement is unlikely to account for the effect: participants actively evaluated the videos, skipping disliked clips on 56.79 ± 19.47 % of trials, indicating sustained involvement rather than generalized disengagement or mind-wandering. Second, given the

passive and hedonic nature of the task, a more plausible explanation is a transition toward automatic, low-effort, immersive processing. Prior research shows that engaging visual media can induce a flow-like state characterized by absorbed attention, diminished self-monitoring, and increased reliance on automatized processing (Alameda et al., 2022; Michailidis et al., 2018). Neurobiologically, such states consistently elicit deactivation within medial prefrontal regions—including areas implicated in monitoring and cognitive control (Ulrich et al., 2016, 2022). Accordingly, the suppression of dACC/dlPFC activity during "liked" video viewing likely reflects an adaptive downregulation that facilitates efficient, immersive engagement rather than a breakdown of control mechanisms.

This interpretation is aligned with our previous research on passive video viewing (Su et al., 2021), where dACC deactivation occurred regardless of video content type (personalized recommendations or general content). We propose that the dACC maintains moderate baseline activity to prepare individuals for potential environmental demands, while excessive baseline activation (as seen in depression; Liu et al., 2014) may impair cognitive control. Reduced dACC/dlPFC engagement during preferred video viewing may thus promote uninterrupted immersion, in line with accounts linking flow states to attenuated frontal activity (Csikszentmihalyi, 2014; Dietrich, 2004; Limb & Braun, 2008). Notably, the dACC and dlPFC exhibit functional divergence. Electrophysiological evidence suggests that the dACC encodes task-related conflicts through neuronal firing rates (Smith et al., 2019), monitoring uncertainty to enable adaptive responses (Fan, 2014), whereas the dlPFC resolves detected conflicts through top-down control (Shenhav et al., 2013, 2017). During "disliked" video viewing, diminished emotional engagement and reward signaling may reduce conflict monitoring demands, allowing dACC activity to return to baseline. In such cases, the dACC may be involved in the initiation of switching to preferred content via motor-related interactions, bypassing dlPFC-involved control. This aligns with the cascade-of-control model, where diminished dlPFC engagement triggers compensatory dACC recruitment (Silton et al., 2010).

4.2. The role of dACC glutamate in cognitive control and neural activation during short video viewing

Previous studies have demonstrated that dACC activation is modulated not only by task states but also by neurotransmitter concentrations (Yücel, Harrison, et al., 2007). In the current study, we identified a positive correlation between the BOLD response during short video viewing and the resting-state glutamate concentration in the dACC. Individuals with elevated baseline glutamate levels in the dACC exhibited relatively higher activation in both the dACC and dlPFC during video viewing, consistent with reduced regional suppression. These findings corroborate earlier research linking ACC glutamate concentrations to task-evoked activation, particularly during empathy-related tasks (Enzi et al., 2012), and extend prior evidence showing that resting-state dACC glutamate concentrations predict BOLD response magnitude during cognitive control tasks (Falkenberg et al., 2012). It is important to note that this relationship is correlational, and while it supports the notion of a link between excitatory neurotransmitter levels and task-evoked BOLD responses, the present data do not permit causal inference regarding the direction of this influence. Together, these results strongly support a reliable association between regional excitatory neurotransmitter concentrations and BOLD signal strength.

The biological basis of the observed association between dACC glutamate concentrations and cognitive control network activation may involve intricate cellular interactions. Higher resting-state regional glutamate concentrations may prime excitatory neurons, amplifying cognitive control network engagement during tasks requiring significant cognitive regulation. Conversely, in contexts with lower cognitive demands, this heightened baseline excitability could manifest as diminished dACC deactivation, reflecting sustained neural activity for ongoing monitoring of decision-making or environmental contingencies. Notably, dACC glutamate concentrations also show associations with activity in distal regions such as the dlPFC. This aligns with observations by Duncan et al. (2014), who reported positive correlations between glutamate levels and neural activity in regions remote from neurotransmitter sampling sites. Such effects may arise from long-range glutamatergic projections (Rockland, 1997), further underscoring the regulatory role of the dACC in cognitive control (Fan, 2014; Shenhav et al., 2013; Smith et al., 2019).

Glutamate and GABA dynamically interact to regulate neuronal excitability and network stability (Sears & Hewett, 2021; Zahid et al., 2023). Although GABAergic inhibition typically suppresses neural activity, prior studies have reported heterogeneous associations between GABA and BOLD signals—including negative, positive, or null correlations (Craven et al., 2024; Hayes et al., 2013; Muthukumaraswamy et al., 2012). This inconsistency suggests that GABA's relationship with neural activation is likely nonlinear and context-dependent, and thus may not be well captured by simple correlational approaches.

Importantly, the absence of a significant association between dACC GABA concentrations and BOLD activity in the current study should not be interpreted as evidence that GABAergic inhibition plays no functional role. MRS-derived GABA predominantly reflects tonic and metabolic pools rather than phasic synaptic release that directly drives fast inhibitory control (Dyke et al., 2017; Rae, 2014). This methodological limitation may reduce sensitivity to detecting GABA–BOLD associations. Additionally, inhibitory influences on prefrontal activity often occur indirectly, such as through modulation of glutamate release or via local interneuron circuits—especially parvalbumin- and somatostatin-positive interneurons—that tightly regulate prefrontal excitability (McGarry & Carter, 2016). Such complex circuit-level mechanisms may interact with glutamatergic drive in ways that obscure linear relationships between regional GABA concentrations and BOLD responses. Future studies employing higher-field MRS or tasks explicitly targeting inhibitory control processes will be necessary to more precisely delineate the contribution of the GABA–glutamate balance to hemodynamic signaling in the dACC.

4.3. Enhanced dACC-dlPFC connectivity during "like" video viewing: implications for cognitive control and conflict adaptation

Our findings demonstrated increased functional connectivity between the dACC and dlPFC during video viewing, with the strongest effects observed when participants watched "liked" videos. The dACC and dlPFC are core components of the cognitive control network, and their coordinated activity is a cornerstone of cognitive control frameworks (Carter et al., 1998; Heilbronner & Hayden, 2016; Voytek et al., 2015; Widge et al., 2019). Although heightened dACC-dlPFC coupling is commonly associated with increased control demands (Clairis & Lopez-Persem, 2023; Fan et al., 2008; Smith et al., 2019), our findings diverge from this classical prediction: connectivity was stronger during the "like" condition, even though both regions exhibited greater deactivation.

A plausible interpretation involves affect-driven modulation of prefrontal dynamics. The amygdala, a central hub in affective processing, is consistently activated during naturalistic emotional movie-watching (Wang et al., 2023). Anatomically, the amygdala influences prefrontal excitability through projections that engage local inhibitory interneurons (Ghashghaei et al., 2007; Grace & Rosenkranz, 2002), exerting a net suppressive effect on both the dACC and dlPFC. We propose that heightened amygdala activity during preferred video viewing may contribute to a shared inhibitory modulation of these regions, leading to joint downregulation of their activity. Under such co-modulation, the residual neural time courses of the dACC and dlPFC may become more temporally aligned, producing increased functional connectivity in PPI analyses. In this view, stronger coupling reflects coordinated disengagement rather than increased engagement of

cognitive control.

By contrast, "disliked" videos likely impose greater monitoring demands, prompting the dACC and dlPFC to engage in more differentiated, task-specific processing. Although both regions are integral to cognitive control, they retain distinct functional specializations (Piretti et al., 2022; Smith et al., 2019). Under high monitoring demands, differential neuronal projections likely drive divergent activation patterns (Silvetti et al., 2018), resulting in weaker temporal correlation and reduced functional connectivity.

Together, these findings suggest that dACC–dlPFC coupling is not exclusively a marker of cognitive control intensity but may also reflect the degree of common modulatory influence, particularly under affectively salient states. This perspective highlights the importance of examining amygdala–prefrontal interactions to fully understand large-scale network dynamics during naturalistic media consumption.

4.4. Limitations and future works

Several limitations should be noted when interpreting these findings. First, neurotransmitter concentrations were not measured in the dlPFC. Given the dlPFC's essential role in cognitive control, future studies should extend metabolite measurements to the dlPFC and explore potential associations between its neurochemical profile and neural activity during short video viewing. Second, the amygdala is integral to reward processing and emotional regulation (Murray, 2007) and shows positive activation during video viewing. Further research is needed to test whether heightened amygdala activity is a causal factor of the dACC and dlPFC deactivation. Third, individual differences in habitual short-video use may substantially influence neural responses. Recent research has shown that individuals with tendencies toward short-video addiction exhibit altered risk-taking behavior, along with structural and functional abnormalities in the frontoparietal control network during both task performance and rest (C. Liu, Li, et al., 2025; C. Liu, Wang, et al., 2025; Yao et al., 2025; S. Zhang & Li, 2025). In the present study, we did not systematically assess participants' compulsive or problematic short-video use. Future studies should incorporate validated short-video addiction or problematic-use scales to determine how usage severity relates to the neural effects identified here. Fourth, the classification of videos as "liked" or "disliked" was based solely on viewing completion (i.e., whether participants watched a video to the end or terminated it early). Although this approach reflects naturalistic browsing behavior—where users commonly signal preference by continuing or skipping—it does not fully disentangle subjective liking from other factors such as video duration, curiosity, or mild engagement. Future studies would benefit from collecting explicit post-viewing ratings to validate whether behavioral skipping decisions correspond to subjective liking. Finally, the long-term consequences of video viewing induced deactivation on cognitive functions like conflict monitoring and resolution remain to be explored, necessitating longitudinal investigations. Moreover, the demographic characteristics of our sample—young, healthy adults with a predominance of male participants— may limit the generalizability of our findings. Prior research has documented sex differences in glutamate/GABA metabolism and media-use patterns, suggesting that neurochemical and functional responses may vary across demographic groups (Laor & Galily, 2022; O'Gorman et al., 2011; Sailasuta et al., 2008; Wu et al., 2025). Future studies with larger, more age- and gender-balanced samples, as well as research involving diverse populations (e.g., children, older adults, or individuals with social disorders, schizophrenia, or depression), will be essential for determining the broader applicability of these results.

5. Conclusion

This study revealed distinct patterns of cognitive control network activity during short video viewing: "liked" videos were associated with significant deactivation in both the dACC and dlPFC, while "disliked" videos elicited stable dACC activity with sustained dlPFC suppression. Resting-state glutamate levels in the dACC were associated with these responses, as higher baseline glutamate correlated with attenuated deactivation in both regions. Functional connectivity between the dACC and dlPFC was significantly enhanced during exposure to "liked" videos compared to "disliked" videos. These findings highlight the critical role of dACC glutamatergic signaling in dynamically shaping cognitive control network flexibility, offering novel insights into neurochemical mechanisms underlying rapid behavioral adaptation to emotionally salient stimuli.

Funding

This work was supported by the National Natural Science Foundation of China (No. 82471511, 81971245, 62077042); the MOE Frontiers Science Center for Brain Science & Brain-Machine Integration, Zhejiang University; Research of Basic Discipline for the 2.0 Base of Top-notch Students Training Program, the Ministry of Education of China (20211033).

Data and code availability statement

Data available on request from the authors.

CRediT authorship contribution statement

Tiantian Hong: Writing – original draft, Visualization, Validation, Investigation, Formal analysis, Data curation, Conceptualization. **Conghui Su:** Software, Methodology, Investigation, Formal analysis, Conceptualization. **Hui Zhou:** Supervision, Conceptualization. **Fengji Geng:** Supervision. **Yuzheng Hu:** Writing – review & editing, Supervision, Funding acquisition.

Declaration of competing interest

None.

Supplementary materials

Supplementary material associated with this article can be found, in the online version, at doi:10.1016/j.neuroimage.2026.121722.

References

Aben, B., Buc Calderon, C., Van Den Bussche, E., Verguts, T., 2020. Cognitive effort modulates connectivity between dorsal anterior cingulate cortex and task-relevant cortical areas. J. Neurosci. 40 (19), 3838–3848. https://doi.org/10.1523/JNEUROSCI.2948-19.2020.

Áfra, E., Janszky, J., Perlaki, G., Orsi, G., Nagy, S.A., Arató, Á., Szente, A., Alhour, H.A. M., Kis-Jakab, G., Darnai, G., 2024. Altered functional brain networks in problematic smartphone and social media use: resting-state fMRI study. Brain Imaging Behav. 18 (2), 292–301. https://doi.org/10.1007/s11682-023-00825-y.

Alameda, C., Sanabria, D., Ciria, L.F., 2022. Brain flow: Syst. Rev. Neural Basis Flow State.

Andrews, P.W., Thomson, J.A., 2009. The bright side of being blue: depression as an adaptation for analyzing complex problems. Psychol. Rev. 116 (3), 620–654. https://doi.org/10.1037/a0016242.

Babür, B.G., Leong, Y.C., Pan, C.X., Hackel, L.M., 2024. Neural responses to social rejection reflect dissociable learning about relational value and reward. Proc. Natl. Acad. Sci. 121 (49), e2400022121. https://doi.org/10.1073/pnas.2400022121.

Baler, R.D., Volkow, N.D., 2006. Drug addiction: the neurobiology of disrupted self-control. Trends Mol. Med. 12 (12), 559–566. https://doi.org/10.1016/j.molmed.2006.10.005.

Botvinick, M., Braver, T., 2015. Motivation and cognitive control: from behavior to neural mechanism. Annu. Rev. Psychol. 66 (1), 83–113. https://doi.org/10.1146/annurev-psych-010814-015044.

Breukelaar, I.A., Antees, C., Grieve, S.M., Foster, S.L., Gomes, L., Williams, L.M., Korgaonkar, M.S., 2017. Cogn. Control Netw. Anat. Correl. Neurocognitive behav.: longitud. Study.

Cadena, E.J., White, D.M., Kraguljac, N.V., Reid, M.A., Maximo, J.O., Nelson, E.A., Gawronski, B.A., Lahti, A.C., 2018. A longitudinal multimodal neuroimaging study to examine relationships between resting State glutamate and task related BOLD

response in schizophrenia. Front. Psychiatry 9, 632. https://doi.org/10.3389/fpsyt.2018.00632.
Carter, C.S., Braver, T.S., Barch, D.M., Botvinick, M.M., Noll, D., Cohen, J.D., 1998. Anterior cingulate cortex, error detection, and the online monitoring of performance. Science 280 (5364), 747–749. https://doi.org/10.1126/science.280.5364.747.
Chen, X., Fan, X., Hu, Y., Zuo, C., Whitfield-Gabrieli, S., Holt, D., Gong, Q., Yang, Y., Pizzagalli, D.A., Du, F., Ongur, D., 2019. Regional GABA concentrations modulate inter-network resting-state functional connectivity. Cereb. Cortex 29 (4), 1607–1618. https://doi.org/10.1093/cercor/bhy059.
Cheng, X., Su, X., Yang, B., Zarifis, A., Mou, J., 2023. Understanding users' negative emotions and continuous usage intention in short video platforms. Electron. Commer. Res. Appl. 58, 101244. https://doi.org/10.1016/j.elerap.2023.101244.
Choi, C., Coupland, N.J., Bhardwaj, P.P., Kalra, S., Casault, C.A., Reid, K., Allen, P.S., 2006. T2 measurement and quantification of glutamate in human brain in vivo. Magn. Reson. Med. 56 (5), 971–977. https://doi.org/10.1002/mrm.21055.
Clairis, N., Barakat, A., Brochard, J., Xin, L., Sandi, C., 2024. A neurometabolic mechanism involving dmPFC/dACC lactate in physical effort-based decision-making. Mol. Psychiatry. https://doi.org/10.1038/s41380-024-02726-y.
Clairis, N., Lopez-Persem, A., 2023. Debates on the dorsomedial prefrontal/dorsal anterior cingulate cortex: insights for future research. Brain 146 (12), 4826–4844. https://doi.org/10.1093/brain/awad263.
Coum, A., Noury, F., Bannier, E., Begriche, K., Fromenty, B., Gandon, Y., Saint-Jalmes, H., Gambarota, G., 2016. The effect of water suppression on the hepatic lipid quantification, as assessed by the LCModel, in a preclinical and clinical scenario. *Magnetic resonance materials in physics*. Biol. Med. 29 (1), 29–37. https://doi.org/10.1007/s10334-015-0508-1.
Cox, R.W., 1996. AFNI: software for analysis and Visualization of Functional Magnetic Resonance Neuroimages. Comput. Biomed. Res. 29 (3), 162–173. https://doi.org/10.1006/cbmr.1996.0014.
Craven, A.R., Dwyer, G., Ersland, L., Kazimierczak, K., Noeske, R., Sandøy, L.B., Johnsen, E., Hugdahl, K., 2024. GABA, glutamatergic dynamics and BOLD contrast assessed concurrently using functional MRS during a cognitive task. NMR Biomed. 37 (3), e5065. https://doi.org/10.1002/nbm.5065.
Csikszentmihalyi, M., 2014. Flow and the Foundations of Positive Psychology: The Collected Works of Mihaly Csikszentmihalyi. Springer, Netherlands. https://doi.org/10.1007/978-94-017-9088-8.
De Joode, N., Van Den Heuvel, O., Koster, M., Clarke, W., Van Balkom, A., Schrantee, A., Vriend, C., 2023. 368. The effect of OCD-symptom provocation on neurometabolites in the lateral occipital cortex and their relation to the BOLD response, a combined fMRS and fMRI paradigm. Biol. Psychiatry 93 (9), S242–S243. https://doi.org/10.1016/j.biopsych.2023.02.608.
Dietrich, A., 2004. Neurocognitive mechanisms underlying the experience of flow. Conscious. Cogn. 13 (4), 746–761. https://doi.org/10.1016/j.concog.2004.07.002.
Ding, Y., Wan, X., Lu, G., Huang, H., Liang, Y., Yu, J., Chen, C., 2022. The associations between smartphone addiction and self-esteem, self-control, and social support among Chinese adolescents: A meta-analysis. Front. Psychol. 13, 1029323. https://doi.org/10.3389/fpsyg.2022.1029323.
Duncan, N.W., Wiebking, C., Northoff, G., 2014. Associations of regional GABA and glutamate with intrinsic and extrinsic neural activity in humans—A review of multimodal imaging studies. Neurosci. Biobehav. Rev. 47, 36–52. https://doi.org/10.1016/j.neubiorev.2014.07.016.
Dyke, K., Pépés, S.E., Chen, C., Kim, S., Sigurdsson, H.P., Draper, A., Husain, M., Nachev, P., Gowland, P.A., Morris, P.G., Jackson, S.R., 2017. Comparing GABA-dependent physiological measures of inhibition with proton magnetic resonance spectroscopy measurement of GABA using ultra-high-field MRI. NeuroImage 152, 360–370. https://doi.org/10.1016/j.neuroimage.2017.03.011.
Edden, R.A.E., Puts, N.A.J., Harris, A.D., Barker, P.B., Evans, C.J., 2014. Gannet: A batch-processing tool for the quantitative analysis of gamma-aminobutyric acid–edited MR spectroscopy spectra. J. Magn. Reson. Imaging 40 (6), 1445–1452. https://doi.org/10.1002/jmri.24478.
Enzi, B., Duncan, N.W., Kaufmann, J., Tempelmann, C., Wiebking, C., Northoff, G., 2012. Glutamate modulates resting state activity in the perigenual anterior cingulate cortex – A combined fMRI–MRS study. Neuroscience 227, 102–109. https://doi.org/10.1016/j.neuroscience.2012.09.039.
Falkenberg, L.E., Westerhausen, R., Specht, K., Hugdahl, K., 2012. Resting-state glutamate level in the anterior cingulate predicts blood-oxygen level-dependent response to cognitive control. Proc. Natl. Acad. Sci. 109 (13), 5069–5073. https://doi.org/10.1073/pnas.1115628109.
Fan, J., 2014. An information theory account of cognitive control. Front. Hum. Neurosci. 8. https://doi.org/10.3389/fnhum.2014.00680.
Fan, J., Hof, P.R., Guise, K.G., Fossella, J.A., Posner, M.I., 2008. The functional integration of the anterior cingulate cortex during conflict processing. Cereb. Cortex 18 (4), 796–805. https://doi.org/10.1093/cercor/bhm125.
Finkelman, T., Furman-Haran, E., Aberg, K.C., Paz, R., Tal, A., 2025. Prefrontal inhibitory mechanisms associated with Putamen activity during valence learning revealed by multimodal fMRI-fMRS. Commun. Biol. 8 (1), 1517. https://doi.org/10.1038/s42003-025-08813-2.
Friston, K.J., Buechel, C., Fink, G.R., Morris, J., Rolls, E., Dolan, R.J., 1997. Psychophysiological and modulatory interactions in neuroimaging. NeuroImage 6 (3), 218–229. https://doi.org/10.1006/nimg.1997.0291.
Fu, Z., Beam, D., Chung, J.M., Reed, C.M., Mamelak, A.N., Adolphs, R., Rutishauser, U., 2022. The geometry of domain-general performance monitoring in the human medial frontal cortex. Science 376 (6593), eabm9922. https://doi.org/10.1126/science.abm9922.
Ganji, S.K., Banerjee, A., Patel, A.M., Zhao, Y.D., Dimitrov, I.E., Browning, J.D., Brown, E.S., Maher, E.A., Choi, C., 2012. T2 measurement of J-coupled metabolites in the human brain at 3T. NMR Biomed. 25 (4). https://doi.org/10.1002/nbm.1767, 10.1002/nbm.1767.
Geng, Y., Gu, J., Wang, J., Zhang, R., 2021. Smartphone addiction and depression, anxiety: the role of bedtime procrastination and self-control. J. Affect. Disord. 293, 415–421. https://doi.org/10.1016/j.jad.2021.06.062.
Geramita, M., Van Der Veen, J.W., Barnett, A.S., Savostyanova, A.A., Shen, J., Weinberger, D.R., Marenco, S., 2011. Reproducibility of prefrontal γ-aminobutyric acid measurements with *J* -edited spectroscopy. NMR Biomed. 24 (9), 1089–1098. https://doi.org/10.1002/nbm.1662.
Ghashghaei, H.T., Hilgetag, C.C., Barbas, H., 2007. Sequence of information processing for emotions based on the anatomic dialogue between prefrontal cortex and amygdala. NeuroImage 34 (3), 905–923. https://doi.org/10.1016/j.neuroimage.2006.09.046.
Grace, A., Rosenkranz, J., 2002. Regulation of conditioned responses of basolateral amygdala neurons. Physiol. Behav. 77 (4–5), 489–493. https://doi.org/10.1016/S0031-9384(02)00909-5.
Haber, S.N., Liu, H., Seidlitz, J., Bullmore, E., 2022. Prefrontal connectomics: from anatomy to human imaging. Neuropsychopharmacology 47 (1), 20–40. https://doi.org/10.1038/s41386-021-01156-6.
Hayes, D.J., Duncan, N.W., Wiebking, C., Pietruska, K., Qin, P., Lang, S., Gagnon, J., BIng, P.G., Verhaeghe, J., Kostikov, A.P., Schirrmacher, R., Reader, A.J., Doyon, J., Rainville, P., Northoff, G., 2013. GABAA receptors predict aversion-related brain responses: an fMRI-PET investigation in healthy humans. Neuropsychopharmacology 38 (8), 1438–1450. https://doi.org/10.1038/npp.2013.40.
Hegarty, J.P., Weber, D.J., Cirstea, C.M., Beversdorf, D.Q., 2018. Cerebro-cerebellar functional connectivity is associated with cerebellar excitation–Inhibition balance in Autism spectrum disorder. J. Autism Dev. Disord. 48 (10), 3460–3473. https://doi.org/10.1007/s10803-018-3613-y.
Heilbronner, S.R., Hayden, B.Y., 2016. Dorsal anterior cingulate cortex: A bottom-up view. Annu. Rev. Neurosci. 39 (1), 149–170. https://doi.org/10.1146/annurev-neuro-070815-013952.
Helfrich, R.F., Knight, R.T., 2016. Oscillatory dynamics of prefrontal cognitive control. Trends Cogn. Sci. 20 (12), 916–930. https://doi.org/10.1016/j.tics.2016.09.007.
Hu, Y., Chen, X., Gu, H., Yang, Y., 2013. Resting-State glutamate and GABA concentrations predict task-induced deactivation in the default mode network. J. Neurosci. 33 (47), 18566–18573. https://doi.org/10.1523/JNEUROSCI.1973-13.2013.
Ip, I.B., Berrington, A., Hess, A.T., Parker, A.J., Emir, U.E., Bridge, H., 2017. Combined fMRI-MRS acquires simultaneous glutamate and BOLD-fMRI signals in the human brain. NeuroImage 155, 113–119. https://doi.org/10.1016/j.neuroimage.2017.04.030.
Kanagasabai, K., Palaniyappan, L., Théberge, J., 2024. Precision of metabolite-selective MRS measurements of glutamate, GABA and glutathione: A review of human brain studies. NMR Biomed. 37 (3), e5071.
Kerns, J.G., Cohen, J.D., MacDonald, A.W., Cho, R.Y., Stenger, V.A., Carter, C.S., 2004. Anterior cingulate conflict monitoring and adjustments in control. Science 303 (5660), 1023–1026. https://doi.org/10.1126/science.1089910.
Kiemes, A., Davies, C., Kempton, M.J., Lukow, P.B., Bennallick, C., Stone, J.M., Modinos, G., 2021. GABA, glutamate and neural activity: A systematic review with meta-analysis of multimodal 1H-MRS-fMRI studies. Front. Psychiatry 12, 644315. https://doi.org/10.3389/fpsyt.2021.644315.
Kreis, R., 2004. Issues of spectral quality in clinical[1] H-magnetic resonance spectroscopy and a gallery of artifacts. NMR Biomed. 17 (6), 361–381. https://doi.org/10.1002/nbm.891.
Laor, T., Galily, Y., 2022. Who'S clicking on on-demand? Media consumption patterns of generations Y & Z. Technol. Soc. 70, 102016. https://doi.org/10.1016/j.techsoc.2022.102016.
Le, T.M., Potvin, S., Zhornitsky, S., Li, C.-S.R., 2021. Distinct patterns of prefrontal cortical disengagement during inhibitory control in addiction: A meta-analysis based on population characteristics. Neurosci. Biobehav. Rev. 127, 255–269. https://doi.org/10.1016/j.neubiorev.2021.04.028.
León Méndez, M., Padrón, I., Fumero, A., Marrero, R.J., 2024. Effects of internet and smartphone addiction on cognitive control in adolescents and young adults: A systematic review of fMRI studies. Neurosci. Biobehav. Rev. 159, 105572. https://doi.org/10.1016/j.neubiorev.2024.105572.
Lesage, E., Sutherland, M.T., Ross, T.J., Salmeron, B.J., Stein, E.A., 2020. Nicotine dependence (trait) and acute nicotinic stimulation (state) modulate attention but not inhibitory control: converging fMRI evidence from Go–Nogo and Flanker tasks. Neuropsychopharmacology 45 (5), 857–865. https://doi.org/10.1038/s41386-020-0623-1.
Limb, C.J., Braun, A.R., 2008. Neural substrates of spontaneous musical performance: an fMRI study of jazz improvisation. PLoS ONE 3 (2), e1679. https://doi.org/10.1371/journal.pone.0001679.
Lin, A., Andronesi, O., Bogner, W., Choi, I., Coello, E., Cudalbu, C., Juchem, C., Kemp, G. J., Kreis, R., Krššák, M., Lee, P., Maudsley, A.A., Meyerspeer, M., Mlynarik, V., Near, J., Öz, G., Peek, A.L., Puts, N.A., Ratai, E., Experts' Working Group on Reporting Standards for MR Spectroscopy, 2021. Minimum Reporting Standards for in vivo Magnetic resonance spectroscopy (MRSinMRS): experts' consensus recommendations. NMR Biomed. 34 (5), e4484. https://doi.org/10.1002/nbm.4484.
Lin, L.-H., Narender, R., Zak, P.J., 2022. Why people keep watching: neurophysiologic immersion during video consumption increases viewing time and influences

behavior. Front. Behav. Neurosci. 16, 1053053. https://doi.org/10.3389/fnbeh.2022.1053053.
Liu, C., Li, H., Shangguan, Q., Zeng, Y., Wang, P., Zhang, Z., Jin, W., Wang, Q., 2025. Neural, psychological, and transcriptomic predictors of short video addiction: A multi-site longitudinal study of fear of missing out and negative affect. NeuroImage 323, 121605. https://doi.org/10.1016/j.neuroimage.2025.121605.
Liu, C., Wang, J., Li, H., Shangguan, Q., Jin, W., Zhu, W., Wang, P., Chen, X., Wang, Q., 2025. Loss aversion and evidence accumulation in short-video addiction: A behavioral and neuroimaging investigation. NeuroImage 313, 121250. https://doi.org/10.1016/j.neuroimage.2025.121250.
Liu, J., Ren, L., Womer, F.Y., Wang, J., Fan, G., Jiang, W., Blumberg, H.P., Tang, Y., Xu, K., Wang, F., 2014. Alterations in amplitude of low frequency fluctuation in treatment-naïve major depressive disorder measured with resting-state fMRI. Hum. Brain Mapp. 35 (10), 4979–4988. https://doi.org/10.1002/hbm.22526.
Long, Z., Medlock, C., Dzemidzic, M., Shin, Y.-W., Goddard, A.W., Dydak, U., 2013. Decreased GABA levels in anterior cingulate cortex/medial prefrontal cortex in panic disorder. Prog. Neuro-Psychopharmacol. Biol. Psychiatry 44, 131–135. https://doi.org/10.1016/j.pnpbp.2013.01.020.
Luijten, M., Machielsen, M., Veltman, D., Hester, R., De Haan, L., Franken, I., 2014. Systematic review of ERP and fMRI studies investigating inhibitory control and error processing in people. J. Psychiatry Neurosci. 39 (3), 149–169. https://doi.org/10.1503/jpn.130052.
Ma, L., Chan, J.L., Johnston, K., Lomber, S.G., Everling, S., 2019. Macaque anterior cingulate cortex deactivation impairs performance and alters lateral prefrontal oscillatory activities in a rule-switching task. PLOS Biol. 17 (7), e3000045. https://doi.org/10.1371/journal.pbio.3000045.
Maner, J.K., Kenrick, D.T., 2010. When adaptations go awry: functional and dysfunctional aspects of social anxiety: adaptations gone awry. Soc. Issues Policy Rev. 4 (1), 111–142. https://doi.org/10.1111/j.1751-2409.2010.01019.x.
Maza, M.T., Fox, K.A., Kwon, S.-J., Flannery, J.E., Lindquist, K.A., Prinstein, M.J., Telzer, E.H., 2023. Association of habitual checking behaviors on social Media with longitudinal functional brain development. JAMA Pediatr. 177 (2), 160. https://doi.org/10.1001/jamapediatrics.2022.4924.
McGarry, L.M., Carter, A.G., 2016. Inhibitory gating of basolateral amygdala inputs to the prefrontal cortex. J. Neurosci. 36 (36), 9391–9406. https://doi.org/10.1523/JNEUROSCI.0874-16.2016.
Michailidis, L., Balaguer-Ballester, E., He, X., 2018. Flow and immersion in video games: the aftermath of a conceptual challenge. Front. Psychol. 9, 1682. https://doi.org/10.3389/fpsyg.2018.01682.
Mlynárik, V., Gruber, S., Moser, E., 2001. Proton T_1 and T_2 relaxation times of human brain metabolites at 3 tesla. NMR Biomed. 14 (5), 325–331. https://doi.org/10.1002/nbm.713.
Mohammadi, H., Zargaran, S.J., Khajehpour, H., Adibi, I., Rahimiforoushani, A., Karimi, S., Serej, N.D., Alam, N.R., 2025. Human short-term memory learning based on dynamic glutamate levels and oscillatory activities: concurrent metabolic and electrophysiological studies using event-related functional-MRS and EEG modalities. Cogn. Process. https://doi.org/10.1007/s10339-025-01317-1.
Mohanty, A., Engels, A.S., Herrington, J.D., Heller, W., Ringo Ho, M., Banich, M.T., Webb, A.G., Warren, S.L., Miller, G.A., 2007. Differential engagement of anterior cingulate cortex subdivisions for cognitive and emotional function. Psychophysiology 44 (3), 343–351. https://doi.org/10.1111/j.1469-8986.2007.00515.x.
Morris, R., Moretta, T., Potenza, M.N., 2023. The psychobiology of problematic use of social Media. Curr. Behav. Neurosci. Rep. 10 (4), 65–74. https://doi.org/10.1007/s40473-023-00261-8.
Mouchlianitis, E.D., Vanes, L.D., Tracy, D.K., Fett, A.-K., Joyce, D., Shergill, S.S., 2023. Neuroimaging glutamatergic mechanisms differentiating antipsychotic treatment-response. Sci. Rep. 13 (1), 8938. https://doi.org/10.1038/s41598-022-26702-0.
Murray, E.A., 2007. The amygdala, reward and emotion. Trends Cogn. Sci. 11 (11), 489–497. https://doi.org/10.1016/j.tics.2007.08.013.
Muthukumaraswamy, S.D., Evans, C.J., Edden, R.A.E., Wise, R.G., Singh, K.D., 2012. Individual variability in the shape and amplitude of the BOLD-HRF correlates with endogenous GABAergic inhibition. Hum. Brain Mapp. 33 (2), 455–465. https://doi.org/10.1002/hbm.21223.
Northoff, G., Walter, M., Schulte, R.F., Beck, J., Dydak, U., Henning, A., Boeker, H., Grimm, S., Boesiger, P., 2007. GABA concentrations in the human anterior cingulate cortex predict negative BOLD responses in fMRI. Nat. Neurosci. 10 (12), 1515–1517. https://doi.org/10.1038/nn2001.
Oboshi, Y., Iwabuchi, T., Takata, Y., Bunai, T., Ouchi, Y., 2025. Cerebellar contribution to emotion regulation and its association with medial frontal GABA level. Soc. Cogn. Affect. Neurosci. 20 (1), nsae091. https://doi.org/10.1093/scan/nsae091.
O'Gorman, R.L., Michels, L., Edden, R.A., Murdoch, J.B., Martin, E., 2011. In vivo detection of GABA and glutamate with MEGA-PRESS: reproducibility and gender effects. J. Magn. Reson. Imaging 33 (5), 1262–1267. https://doi.org/10.1002/jmri.22520.
Overbeek, G., Gawne, T.J., Reid, M.A., Salibi, N., Kraguljac, N.V., White, D.M., Lahti, A. C., 2019. Relationship between cortical excitation and inhibition and task-induced activation and deactivation: A combined magnetic resonance spectroscopy and functional magnetic resonance imaging study at 7T in first-episode psychosis. Biol. Psychiatry: Cogn. Neurosci. Neuroimaging 4 (2), 121–130. https://doi.org/10.1016/j.bpsc.2018.10.002.
Petrides, M., Pandya, D.N., 1999. Dorsolateral prefrontal cortex: comparative cytoarchitectonic analysis in the human and the macaque brain and corticocortical connection patterns. Eur. J. Neurosci. 11 (3), 1011–1036. https://doi.org/10.1046/j.1460-9568.1999.00518.x.
Piretti, L., Pappaianni, E., Gobbo, S., Rumiati, R.I., Job, R., Grecucci, A., 2022. Dissociating the role of dACC and dlPFC for emotion appraisal and mood regulation using cathodal tDCS. Cogn. Affect. Behav. Neurosci. 22 (2), 304–315. https://doi.org/10.3758/s13415-021-00952-3.
Power, J.D., Barnes, K.A., Snyder, A.Z., Schlaggar, B.L., Petersen, S.E., 2012. Spurious but systematic correlations in functional connectivity MRI networks arise from subject motion. NeuroImage 59 (3), 2142–2154. https://doi.org/10.1016/j.neuroimage.2011.10.018.
Provencher, S., 2021. LCModel1 LCMgui User's Man.
Provencher, S.W., 1993. Estimation of metabolite concentrations from localized in vivo proton NMR spectra. Magn. Reson. Med. 30 (6), 672–679. https://doi.org/10.1002/mrm.1910300604.
Rae, C.D., 2014. A guide to the metabolic pathways and function of metabolites observed in Human brain 1H magnetic resonance spectra. Neurochem. Res. 39 (1), 1–36. https://doi.org/10.1007/s11064-013-1199-5.
Rigby, J.M., Brumby, D.P., Cox, A.L., Gould, S.J.J., 2016. Watching movies on netflix: investigating the effect of screen size on viewer immersion. In: Proceedings of the 18th International Conference on Human-Computer Interaction with Mobile Devices and Services Adjunct, pp. 714–721. https://doi.org/10.1145/2957265.2961843.
Ritz, H., Shenhav, A., 2024. Orthogonal neural encoding of targets and distractors supports multivariate cognitive control. Nat. Hum. Behav. https://doi.org/10.1038/s41562-024-01826-7.
Rockland, K.S., 1997. Elements of cortical architecture. In: Rockland, K.S., Kaas, J.H., Peters, A. (Eds.), Extrastriate Cortex in Primates. Springer US, pp. 243–293. https://doi.org/10.1007/978-1-4757-9625-4_6.
Sailasuta, N., Ernst, T., Chang, L., 2008. Regional variations and the effects of age and gender on glutamate concentrations in the human brain. Magn. Reson. Imaging 26 (5), 667–675. https://doi.org/10.1016/j.mri.2007.06.007.
Saleh, M.G., Near, J., Alhamud, A., Robertson, F., Van Der Kouwe, A.J.W., Meintjes, E. M., 2016. Reproducibility of macromolecule suppressed GABA measurement using motion and shim navigated MEGA-SPECIAL with LCModel, jMRUI and GANNET. Magn. Reson. Mater. Phys. Biol. Med. 29 (6), 863–874. https://doi.org/10.1007/s10334-016-0578-8.
Sears, S.M., Hewett, S.J., 2021. Influence of glutamate and GABA transport on brain excitatory/inhibitory balance. Exp. Biol. Med. 246 (9), 1069–1083. https://doi.org/10.1177/1535370221989263.
Shenhav, A., Botvinick, M.M., Cohen, J.D., 2013. The expected value of control: an integrative theory of anterior cingulate cortex function. Neuron 79 (2), 217–240. https://doi.org/10.1016/j.neuron.2013.07.007.
Shenhav, A., Cohen, J.D., Botvinick, M.M., 2016. Dorsal anterior cingulate cortex and the value of control. Nat. Neurosci. 19 (10), 1286–1291. https://doi.org/10.1038/nn.4384.
Shenhav, A., Musslick, S., Lieder, F., Kool, W., Griffiths, T.L., Cohen, J.D., Botvinick, M. M., 2017. Toward a rational and mechanistic account of mental effort. Annu. Rev. Neurosci. 40 (1), 99–124. https://doi.org/10.1146/annurev-neuro-072116-031526.
Sheth, S.A., Mian, M.K., Patel, S.R., Asaad, W.F., Williams, Z.M., Dougherty, D.D., Bush, G., Eskandar, E.N., 2012. Human dorsal anterior cingulate cortex neurons mediate ongoing behavioural adaptation. Nature 488 (7410), 218–221. https://doi.org/10.1038/nature11239.
Silton, R.L., Heller, W., Towers, D.N., Engels, A.S., Spielberg, J.M., Edgar, J.C., Sass, S.M., Stewart, J.L., Sutton, B.P., Banich, M.T., Miller, G.A., 2010. The time course of activity in dorsolateral prefrontal cortex and anterior cingulate cortex during top-down attentional control. NeuroImage 50 (3), 1292–1302. https://doi.org/10.1016/j.neuroimage.2009.12.061.
Silvestrini, N., Musslick, S., Berry, A.S., Vassena, E., 2023. An integrative effort: bridging motivational intensity theory and recent neurocomputational and neuronal models of effort and control allocation. Psychol. Rev. 130 (4), 1081–1103. https://doi.org/10.1037/rev0000372.
Silvetti, M., Vassena, E., Abrahamse, E., Verguts, T., 2018. Dorsal anterior cingulate-brainstem ensemble as a reinforcement meta-learner. PLOS Comput. Biol. 14 (8), e1006370. https://doi.org/10.1371/journal.pcbi.1006370.
Simpson, R., Devenyi, G.A., Jezzard, P., Hennessy, T.J., Near, J., 2017. Advanced processing and simulation of MRS data using the FID appliance (FID-A)—An open source, MATLAB-based toolkit. Magn. Reson. Med. 77 (1), 23–33. https://doi.org/10.1002/mrm.26091.
Smith, E.H., Banks, G.P., Mikell, C.B., Cash, S.S., Patel, S.R., Eskandar, E.N., Sheth, S.A., 2015. Frequency-dependent representation of reinforcement-related information in the Human medial and lateral prefrontal cortex. J. Neurosci. 35 (48), 15827–15836. https://doi.org/10.1523/JNEUROSCI.1864-15.2015.
Smith, E.H., Horga, G., Yates, M.J., Mikell, C.B., Banks, G.P., Pathak, Y.J., Schevon, C.A., McKhann, G.M., Hayden, B.Y., Botvinick, M.M., Sheth, S.A., 2019. Widespread temporal coding of cognitive control in the human prefrontal cortex. Nat. Neurosci. 22 (11), 1883–1891. https://doi.org/10.1038/s41593-019-0494-0.
Song, S., Zilverstand, A., Song, H., d'Oleire Uquillas, F., Wang, Y., Xie, C., Cheng, L., Zou, Z., 2017. The influence of emotional interference on cognitive control: A meta-analysis of neuroimaging studies using the emotional Stroop task. Sci. Rep. 7 (1), 2088. https://doi.org/10.1038/s41598-017-02266-2.
Srinivasan, R., Cunningham, C., Chen, A., Vigneron, D., Hurd, R., Nelson, S., Pelletier, D., 2006. TE-averaged two-dimensional proton spectroscopic imaging of glutamate at 3 T. NeuroImage 30 (4), 1171–1178. https://doi.org/10.1016/j.neuroimage.2005.10.048.
Su, C., Teng, B., Zhou, H., Geng, F., Hu, Y., 2023. Prefrontal Suppr. Short-video viewing: Unraveling Neural Correl. Self-Control. https://doi.org/10.1101/2023.10.30.23296738.
Su, C., Zhou, H., Gong, L., Teng, B., Geng, F., Hu, Y., 2021. Viewing personalized video clips recommended by TikTok activates default mode network and ventral tegmental

area. NeuroImage 237, 118136. https://doi.org/10.1016/j.neuroimage.2021.118136.
Swanson, J., Moyzis, R., Fossella, J., Fan, J., Posner, M.I., 2002. Adaptationism and molecular biology: an example based on ADHD. Behav. Brain Sci. 25 (04). https://doi.org/10.1017/S0140525X02490097.
Ulrich, M., Keller, J., Grön, G., 2016. Neural signatures of experimentally induced flow experiences identified in a typical fMRI block design with BOLD imaging. Soc. Cogn. Affect. Neurosci. 11 (3), 496–507. https://doi.org/10.1093/scan/nsv133.
Ulrich, M., Niemann, F., Grön, G., 2022. Role of the right anterior insula for the emergence of flow—A combined task-based fMRI activation and connectivity study. Front. Hum. Neurosci. 16, 1067968. https://doi.org/10.3389/fnhum.2022.1067968.
Voytek, B., Kayser, A.S., Badre, D., Fegen, D., Chang, E.F., Crone, N.E., Parvizi, J., Knight, R.T., D'Esposito, M., 2015. Oscillatory dynamics coordinating human frontal networks in support of goal maintenance. Nat. Neurosci. 18 (9), 1318–1324. https://doi.org/10.1038/nn.4071.
Wang, L., Hu, X., Ren, Y., Lv, J., Zhao, S., Guo, L., Liu, T., Han, J., 2023. Arousal modulates the amygdala-insula reciprocal connectivity during naturalistic emotional movie watching. NeuroImage 279, 120316. https://doi.org/10.1016/j.neuroimage.2023.120316.
Widge, A.S., Heilbronner, S.R., Hayden, B.Y., 2019. Prefrontal cortex and cognitive control: new insights from human electrophysiology. F1000Research 8, 1696. https://doi.org/10.12688/f1000research.20044.1.
Wijtenburg, S.A., Rowland, L.M., Edden, R.A.E., Barker, P.B., 2013. Reproducibility of brain spectroscopy at 7T using conventional localization and spectral editing techniques. J. Magn. Reson. Imaging 38 (2), 460–467. https://doi.org/10.1002/jmri.23997.
Windischberger, C., Langenberger, H., Sycha, T., Tschernko, E.M., Fuchsjäger-Mayerl, G., Schmetterer, L., Moser, E., 2002. On the origin of respiratory artifacts in BOLD-EPI of the human brain. Magnet. Reson. Imag. 20 (8), 575–582.
Woo, J.H., Azab, H., Jahn, A., Hayden, B., Brown, J.W., 2022. The PRO model accounts for the anterior cingulate cortex role in risky decision-making and monitoring. Cogn. Affect. Behav. Neurosci. 22 (5), 952–968. https://doi.org/10.3758/s13415-022-00992-3.
Wu, Y., Bai, Y., Liu, X., Xu, W., Liu, Y., 2025. Gender differences in the relationship between short-form video addiction and adolescent depression: the mediating role of attentional bias. Cyberpsychology Behav. Soc. Netw. 28 (3), 169–177. https://doi.org/10.1089/cyber.2024.0442.
Yao, Q., Gao, Y., Liu, C., Li, X., Jin, W., Wang, Q., 2025. The impact of childhood trauma on short video addiction: psychological and morphological correlates. Sci. Rep. 15 (1), 18999. https://doi.org/10.1038/s41598-025-04020-5.
Yücel, M., Harrison, B.J., Wood, S.J., Fornito, A., Clarke, K., Wellard, R.M., Cotton, S., Pantelis, C., 2007. State, trait and biochemical influences on human anterior cingulate function. NeuroImage 34 (4), 1766–1773. https://doi.org/10.1016/j.neuroimage.2006.08.057.
Yücel, M., Lubman, D.I., Harrison, B.J., Fornito, A., Allen, N.B., Wellard, R.M., Roffel, K., Clarke, K., Wood, S.J., Forman, S.D., Pantelis, C., 2007. A combined spectroscopic and functional MRI investigation of the dorsal anterior cingulate region in opiate addiction. Mol. Psychiatry 12 (7), 691–702. https://doi.org/10.1038/sj.mp.4001955.
Zahid, U., Onwordi, E.C., Hedges, E.P., Wall, M.B., Modinos, G., Murray, R.M., Egerton, A., 2023. Neurofunctional correlates of glutamate and GABA imbalance in psychosis: A systematic review. Neurosci. Biobehav. Rev. 144, 105010. https://doi.org/10.1016/j.neubiorev.2022.105010.
Zhang, N., Hazarika, B., Chen, K., Shi, Y., 2023. A cross-national study on the excessive use of short-video applications among college students. Comput. Hum. Behav. 145, 107752. https://doi.org/10.1016/j.chb.2023.107752.
Zhang, S., Li, S., 2025. How short video addiction affects risk decision-making behavior in college students based on fNIRS technology. Front. Hum. Neurosci. 19, 1542271. https://doi.org/10.3389/fnhum.2025.1542271.